Electronic Supplementary Information

Quantum Yield in Blue-Emitting Anthracene Derivatives: Vibronic Coupling Density and Transition Dipole Moment Density

Motoyuki Uejima,[a] Tohru Sato,[*a,b] Daisuke Yokoyama,[c] Kazuyoshi Tanaka,[a] and Jong-Wook Park[d]

May 7, 2014

[a] *Department of Molecular Engineering, Graduate School of Engineering, Kyoto University, Nishikyo-ku, Kyoto 615-8510, Japan Tel: +81-75-383-2803; Fax: +81-75-383-2555; E-mail: tsato@scl.kyoto-u.ac.jp*

[b] *Unit of Elements Strategy Initiative for Catalysts & Batteries, Kyoto University, Nishikyo-ku, Kyoto 615-8510, Japan*

[c] *Department of Organic Device Engineering and Research Center of Organic Electronics (ROEL), Yamagata University, 4-3-16 Jonan, Yonezawa, Yamagata 992-8510, Japan*

[d] *Department of Chemistry/Display Research Center, The Catholic University of Korea, Bucheon 420-743, Republic of Korea*

Contents

S1 Duschinsky Effect **3**

S2 Off-Diagonal Vibronic Coupling Density Analysis **4**

S3 Potential Energy Surfaces in the Torsional Distortion **10**

S3.1 Potential energy surface for MADN 10

S3.2 Potential energy surface for MAM 11

S3.3 Potential energy surface for MAT 12

S1 Duschinsky Effect

The Duschinsky effect[1] arises when the normal modes in the excited and ground states are different.[2] The normal modes for the two electronic states are connected by the Duschinsky rotation matrix **D** as

$$Q_{n,\alpha} = T_{n,\alpha} + \sum_{\beta} D_{n,\alpha\beta} Q_{\beta}, \tag{1}$$

where $Q_{n,\alpha}$ denotes the normal mode in the S_n state, $T_{n,\alpha}$ is an element of the displacement vector connecting the minima of the parabola of the S_n and S_0 states, and $D_{n,\alpha\beta}$ is the matrix element of **D**. The quadratic VCCs in the S_n state is defined by

$$W_{n,\alpha\beta} = \left\langle \Psi_n(\mathbf{r},\mathbf{R}_0) \left| \left(\frac{\partial^2 H}{\partial Q_\alpha Q_\beta} \right)_{\mathbf{R}_0} \right| \Psi_n(\mathbf{r},\mathbf{R}_0) \right\rangle. \tag{2}$$

The normal modes and their frequencies in the excited states can be obtained by the diagonalization of the quadratic vibronic couplings:

$$\sum_{\beta} W_{n,\alpha\beta} Q_{n,\beta} = \sum_{\beta} \omega_{n,\alpha}^2 \delta_{\alpha\beta} Q_{n,\beta} \tag{3}$$

Now, we introduce the quadratic VCC difference between the S_n and S_0 states defined by $\Delta W_{\alpha\beta} := W_{n,\alpha\beta} - W_{0,\alpha\beta}$. Using the first order perturbation approximation, the normal mode in the excited state is given by

$$Q_{n,\alpha} = \sum_{\beta\neq\alpha} \frac{\Delta W_{n,\alpha\beta}}{\omega_\beta - \omega_\alpha} Q_\beta. \tag{4}$$

Therefore, the off-diagonal matrix elements of **D** is written as

$$D_{n,\alpha\beta} \approx \frac{\Delta W_{n,\alpha\beta}}{\omega_\beta - \omega_\alpha} \qquad (\beta \neq \alpha) \tag{5}$$

The quadratic VCC difference $\Delta W_{\alpha\beta}$ is expressed as the integration of the product of the quadratic potential derivative $w_{\alpha\beta}$ and electron-density difference $w_{\alpha\beta}$:[3]

$$\Delta W_{n,\alpha\beta} = \int w_{\alpha\beta}(r) \Delta\rho_n(r) d^3r. \tag{6}$$

As is the case with the VCD analysis, we can analyze the Duschinsky effect via the electron-density difference.

As shown in Figures 3(c) and 6(c), the electron-density differences are strongly localized on the anthracene moieties. Therefore the Duschinsky rotation also primarily originates from the anthracene moieties. If the normal modes are localized on the side moieties, the potential derivative $w_{\alpha\beta}$ does not overlap with the electron-density difference. In other words, the Duschinsky rotation matrix element is small.

In the previous study, we confirmed the Duschinsky effect is negligible in the anthracene.[4] The Duschinsky effect of the low-frequency mode is rather large, but those of the other modes are small. Since the off-diagonal and diagonal VCCs of the low-frequency mode are small, the Duschinsky effect does not significantly affect the vibronic effects in these system.

S2 Off-Diagonal Vibronic Coupling Density Analysis

Figure S1 shows the the maximum-coupling modes of the off-diagonal VCCs. Figure S2 shows the derivatives of the nuclear-electronic potential with respect to the maximum-coupling modes v_α. Because the core moiety of MADN includes a methyl group, the C(13) and C(14) atoms do not stretch along to the C(13) - C(14) bond, as shown in Fig. S1(a). For this reason, the distribution of v_α on the C(13) and C(14) atoms for MADN is different from that of the other molecules.

The overlap densities between the S_1 and S_0 states ρ_{01} are shown in Fig. S3. The overlap densities are mainly localized on the anthracenylene groups. The distributions of ρ_{01} in all the molecules are almost symmetric around the C(9) and C(10) atoms.

The off-diagonal vibronic coupling densities $\eta_{01,\alpha}$ are shown in Fig. S4. The vibronic coupling densities $\eta_{01,\alpha}$ are mainly localized on the anthracenylene groups. The localized $\eta_{01,\alpha}$'s on the anthracenylene groups come from the localization of ρ_{01}. Cancellations of $\eta_{01,\alpha}$ occur around the C(9) and C(10) atoms in the spatial integration of $\eta_{01,\alpha}$ because ρ_{01}'s are distributed symmetrically on these two atoms. $\eta_{01,\alpha}$ around the C(11) - C(14) atoms is large because v_α around the four atoms is large.

Figure S5 shows the off-diagonal AVCCs between the S_1 and S_0 states for the maximum-coupling mode of MADN, MAT, and TAT, and for the second maximum coupling mode of MAM in the core moiety. For each molecule, the off-diagonal AVCCs for the C(9) and C(10) atoms are small because of the cancellations in the spatial integration of $\eta_{01,\alpha}$. It is found that the off-diagonal AVCCs for the C(11) - C(14) atoms are the largest in TAT and MAM because there is cancellation. On the other hand, there exist two large off-diagonal AVCCs in MAT and MADN: the off-diagonal AVCCs for the C(12) and C(14) atoms are the largest in MADN, and those for the C(13) and C(14) atoms are the largest in MAT. The off-diagonal AVCC for the other atoms are small because $\eta_{01,\alpha}$'s are cancelled in the spatial integration around these atoms. Thus, the cancellations give rise to smaller off-diagonal VCCs for MADN and MAT than those for MAM and TAT.

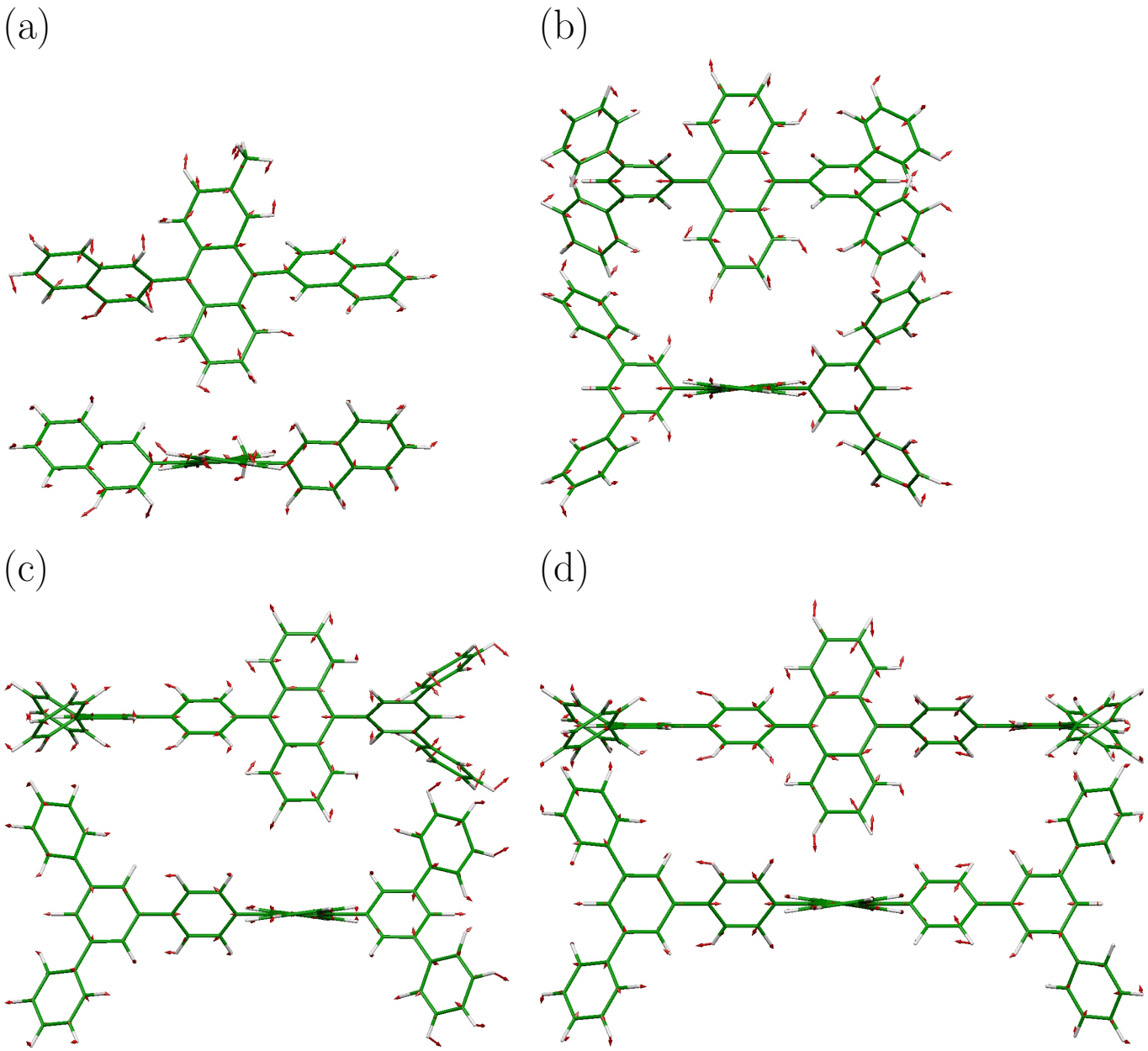

Fig. S1 Maximum-coupling modes for MADN, MAT, and TAT, and second maximum coupling mode for MAM: (a) MADN ($\omega_{47} = 666.38$ cm^{-1}), (b) MAM ($\omega_{88} = 819.81$ cm^{-1}), (c) MAT ($\omega_{97} = 792.55$ cm^{-1}), and (d) TAT ($\omega_{98} = 742.02$ cm^{-1}).

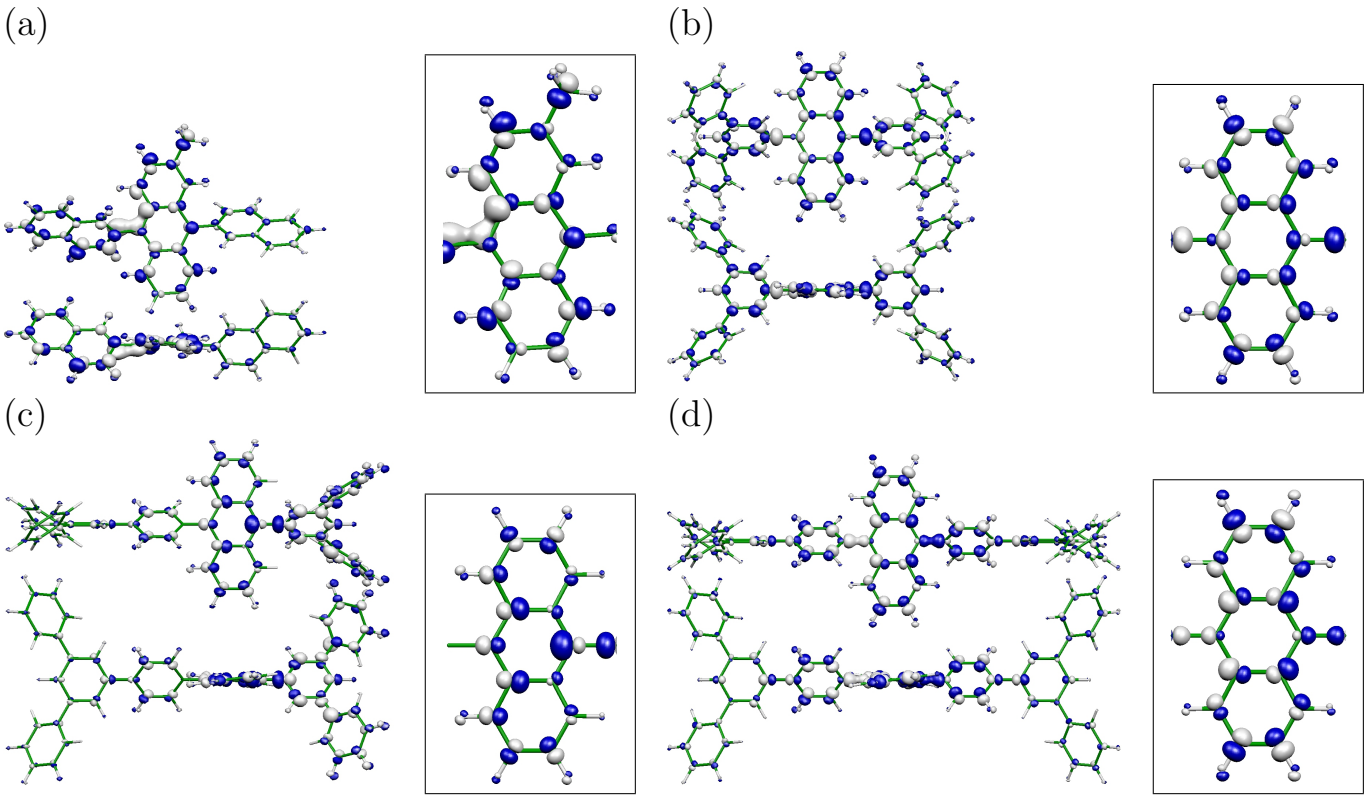

Fig. S2 Derivatives of the nuclear-electronic potential with respect to the maximum-coupling modes of the off-diagonal VCCs for MADN, MAT, and TAT, and to the second maximum coupling mode of the off-diagonal VCC for MAM: (a) MADN (ν_{47}), (b) MAM (ν_{88}), (c) MAT (ν_{97}), and (d) TAT (ν_{98}). The isosurface value is 8×10^{-3} a.u. Blue regions are negative; white regions are positive.

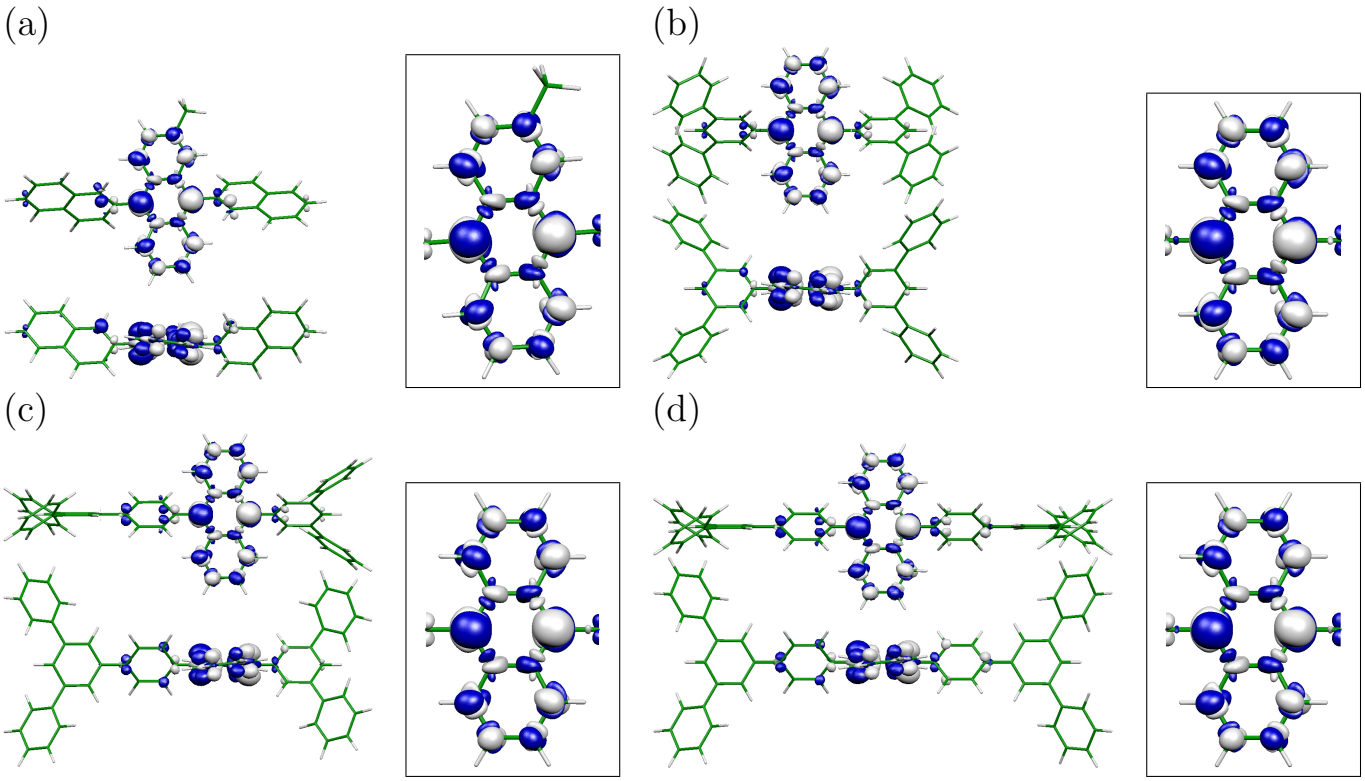

Fig. S3 Overlap densities between the S_1 and S_0 states ρ_{01}: (a) MADN, (b) MAM, (c) MAT, and (d) TAT. The isosurface value is 2×10^{-3} a.u. Blue regions are negative; white regions are positive.

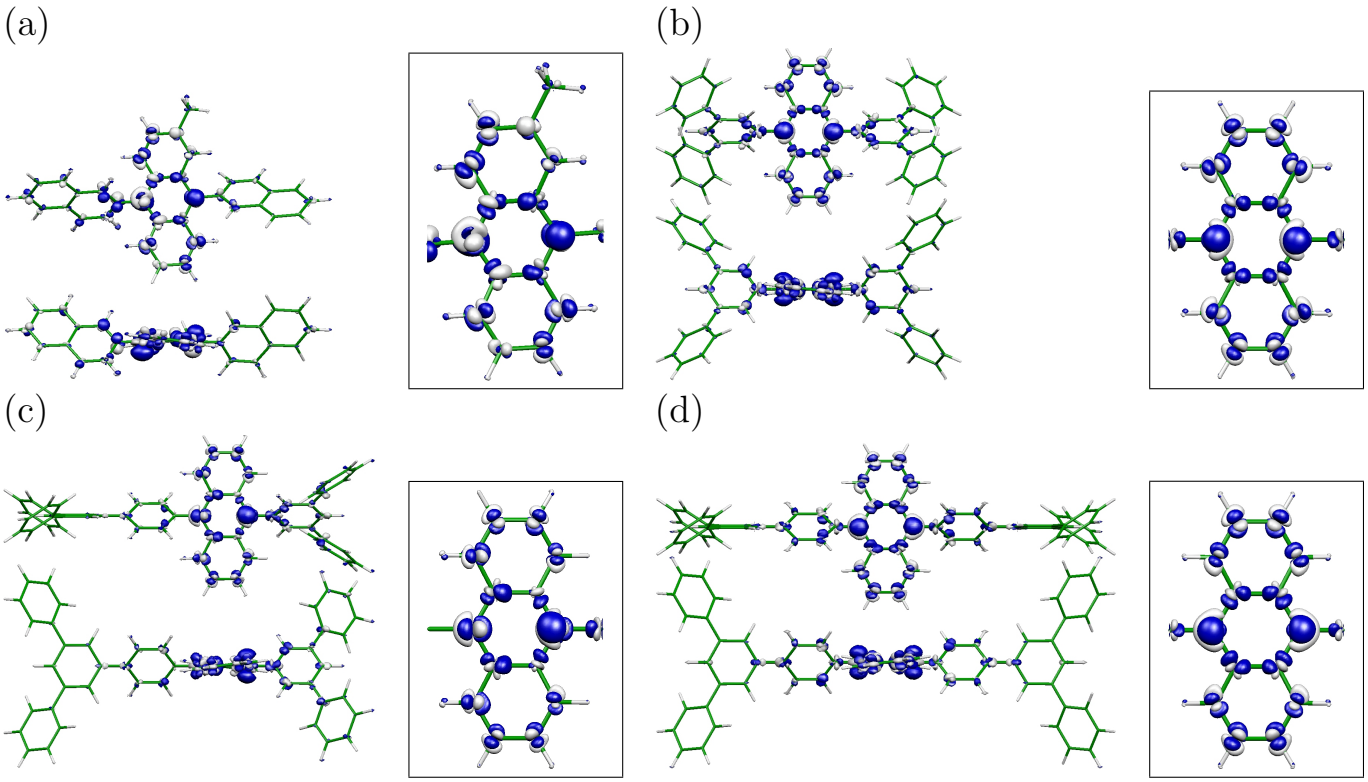

Fig. S4 Off-diagonal vibronic coupling densities between the S_1 and S_0 states: (a) MADN ($\eta_{01,47}$), (b) MAM ($\eta_{01,88}$), (c) MAT ($\eta_{01,97}$), and (d) TAT ($\eta_{01,98}$). The isosurface value is 1×10^{-5} a.u. Blue regions are negative; white regions are positive.

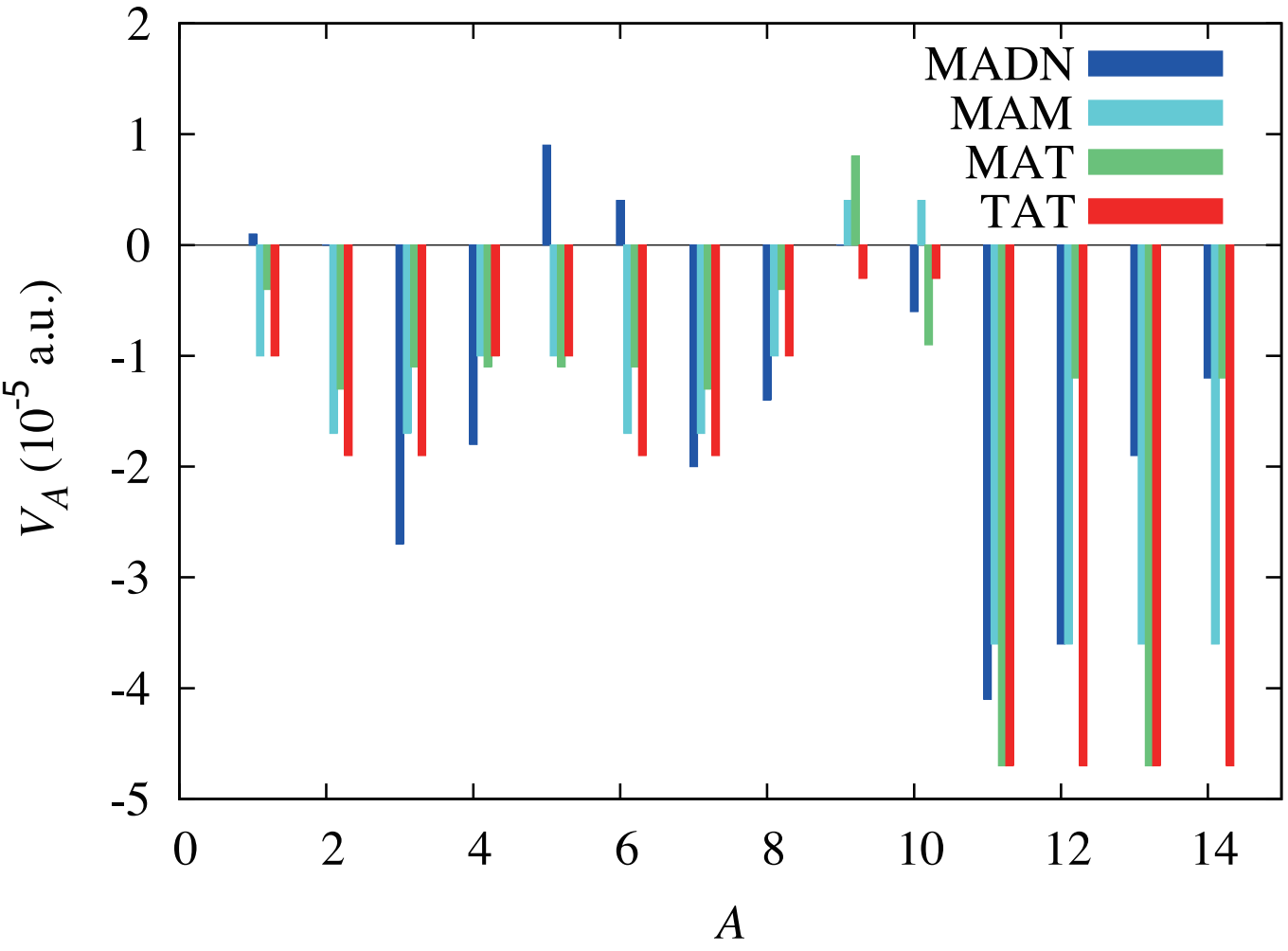

Fig. S5 Off-diagonal atomic vibronic coupling constants between the S_1 and S_0 states for the maximum-coupling mode of MADN, MAT, and TAT, and for the second maximum coupling mode of MAM in the core moiety.

S3 Potential Energy Surfaces in the Torsional Distortion

S3.1 Potential energy surface for MADN

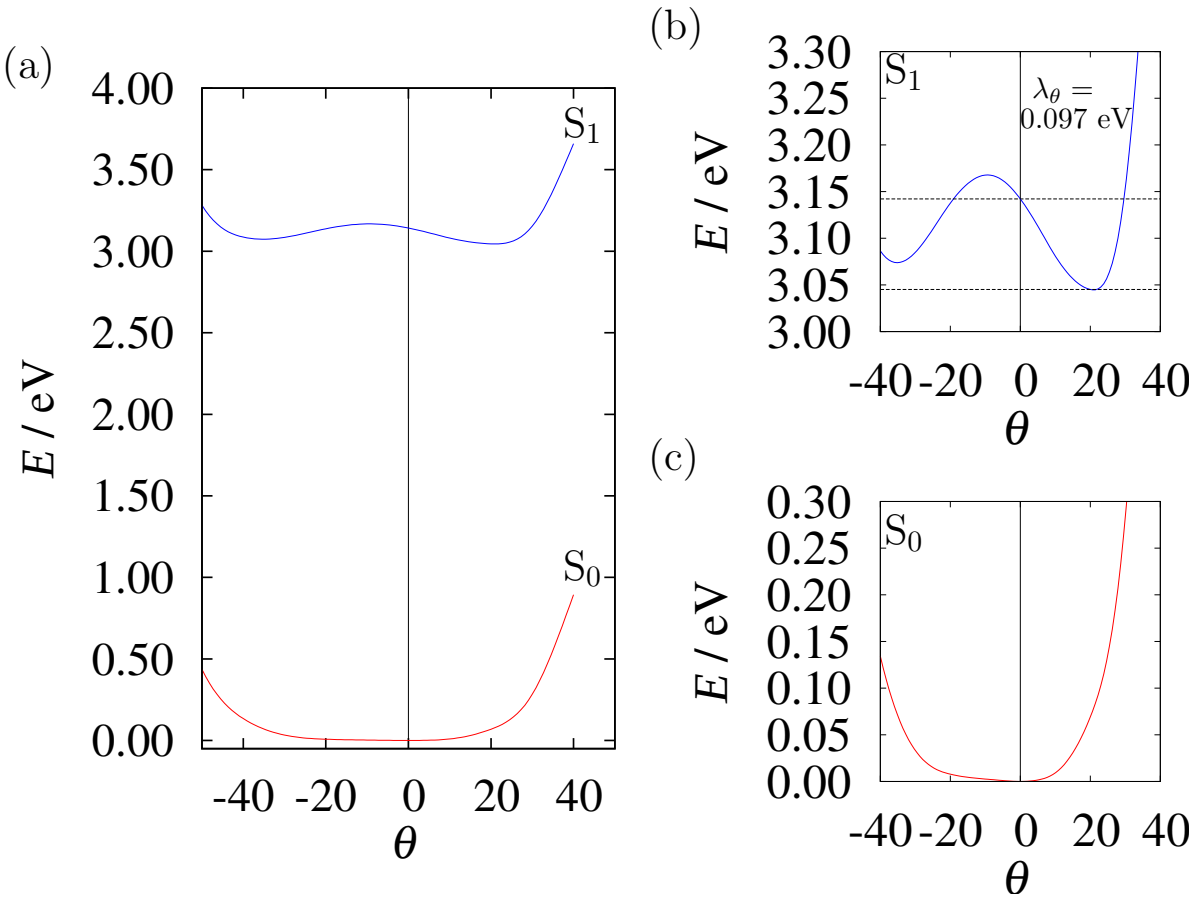

Fig. S6 Potential energy curves for MADN in the twist angle θ: (a) overview; (b) enlarged view for S_1; and (c) enlarged view for S_0. The twist angle θ is defined as the twist angle of the side-moieties of the molecules from the structure in the Franck-Condon state, as shown in Fig. 11. λ_θ represents the reorganization energy for the twist of the side group.

S3.2 Potential energy surface for MAM

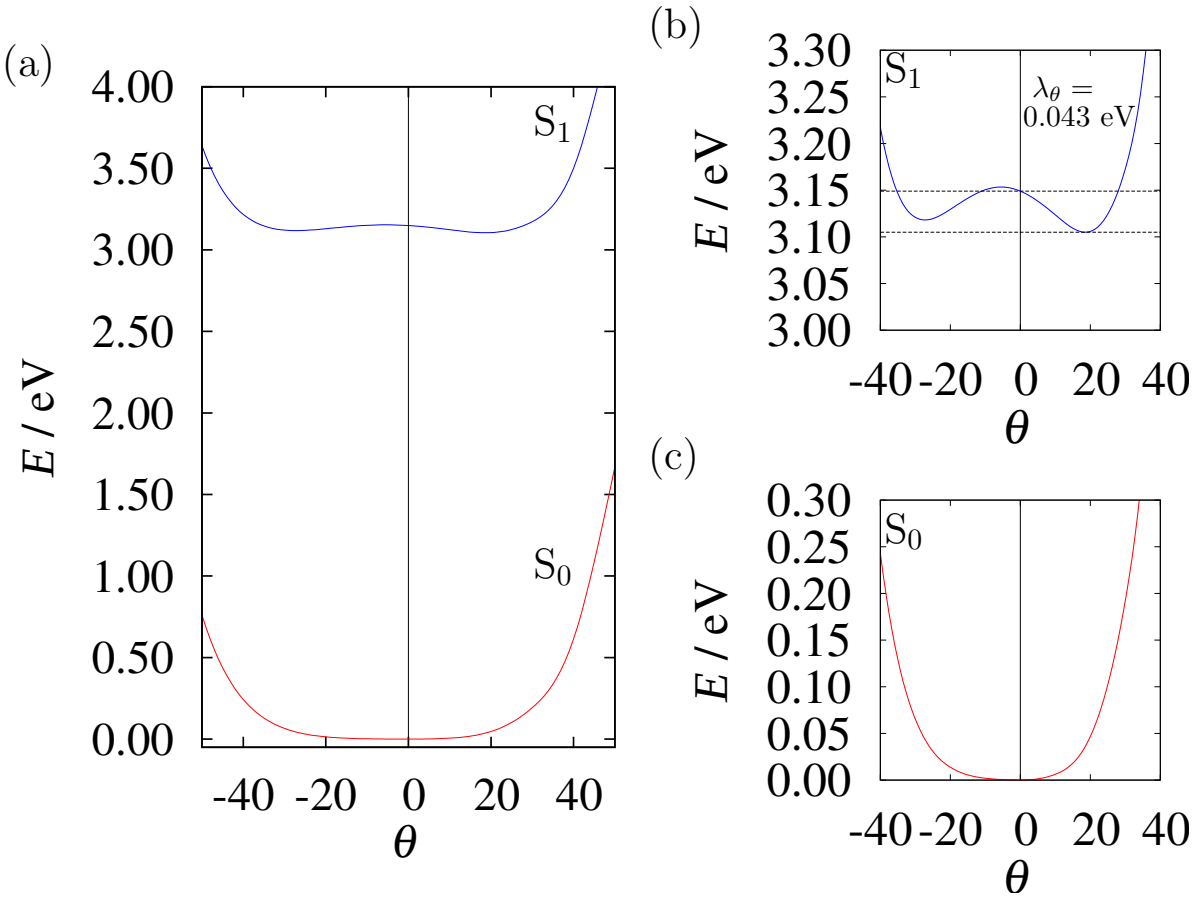

Fig. S7 Potential energy curves for MAM in the twist angle θ: (a) overview; (b) enlarged view for S_1; and (c) enlarged view for S_0. The twist angle θ is defined as the twist angle of the side-moieties of the molecules from the structure in the Franck-Condon state, as shown in Fig. 11. λ_θ represents the reorganization energy for the twist of the side group.

S3.3 Potential energy surface for MAT

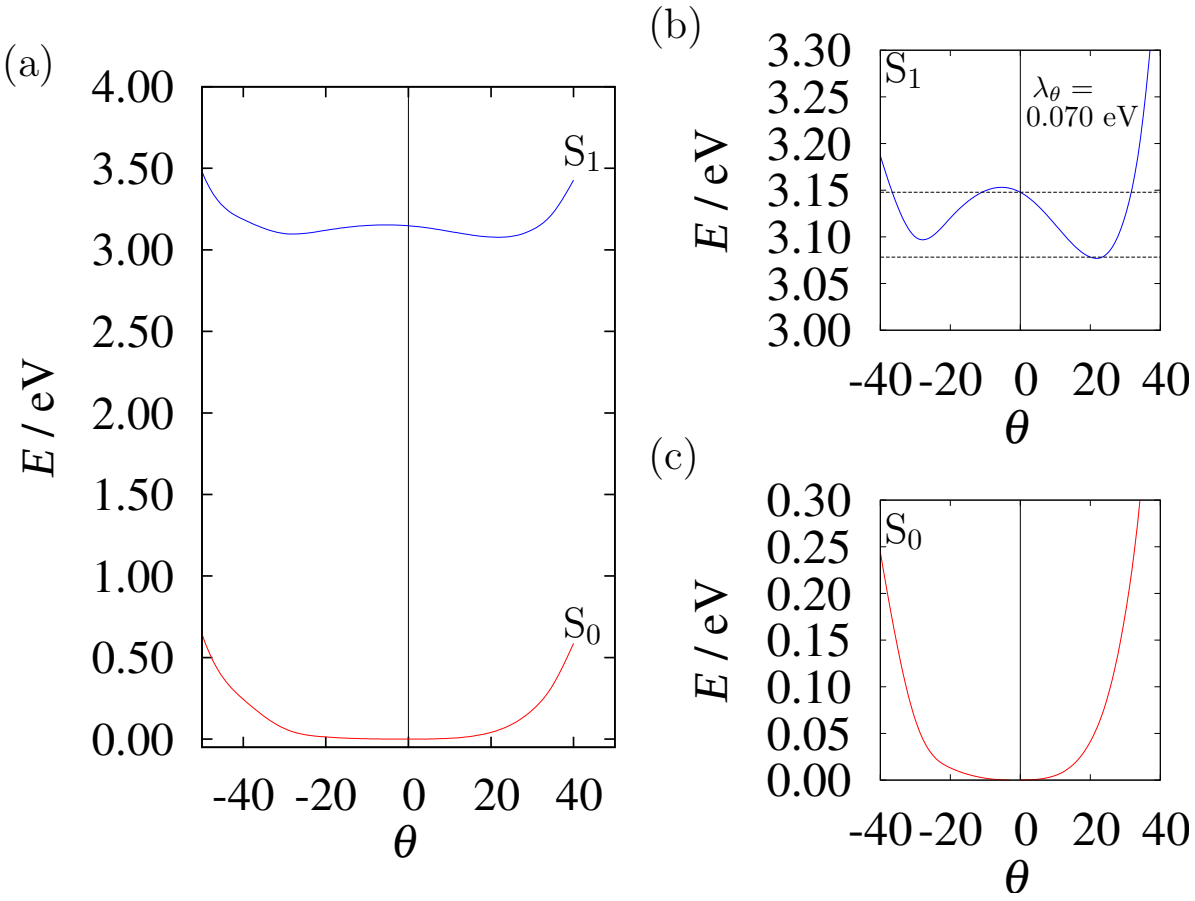

Fig. S8 Potential energy curves for MAT in the twist angle θ: (a) overview; (b) enlarged view for S_1; and (c) enlarged view for S_0. The twist angle θ is defined as the twist angle of the side-moieties of the molecules from the structure in the Franck-Condon state, as shown in Fig. 11. λ_θ represents the reorganization energy for the twist of the side group.

References

1 F. Duschinsky, *F. Duschinsky, Acta Physicochimica U.R.S.S.*, 1937, **7**, 551–566.

2 G. Fischer, *Vibronic Coupling: The Interaction Between the Electronic and Nuclear Motions*, Academic Press, London, 1984.

3 T. Sato, M. Uejima, N. Iwahara, N. Haruta, K. Shizu and K. Tanaka, *J. Phys.: Conf. Ser.*, 2013, **428**, 012010(1–19).

4 M. Uejima, T. Sato, K. Tanaka and H. Kaji, *Chem. Phys.*, 2014, **430**, 47–55.